Earthquake Simulation Tests on a 1:5 Scale 10 - Story RC Residential Building Model

H. S. Lee, S. J. Hwang, K. B. Lee, & C. B. Kang
Korea University, Seoul, Republic of Korea

S. H. Lee & S. H. Oh
Pusan National University, Busan, Republic of Korea

SUMMARY:
This paper presents the results of earthquake simulation tests on a 1:5 scale 10-story RC wall-type residential building model. The following conclusions are drawn based on the test results; (1) The values of base shear coefficients (C_S) under 0.374XY (design earthquake, DE) and 0.60XY (maximum considered earthquake, MCE) are in between design spectra corresponding to the values of response modification factors (R), 1 and 3. The demand under the MCE is approximately 1.5 times larger than that under the DE. The nonlinear relation between the base shear coefficient and the roof drift can be noticed with the over-strength factors under the DE (0.374XY) being approximately 2.0 in the X direction and 1.5 in the Y direction, respectively, when compared with the design seismic load. (2) The maximum inter-story drift (ID) is 1.8mm in the X direction and 1.85mm in the Y direction at the first story under the design earthquake (0.374XY). It can be found that these ID's are far smaller than the ID limit given in KBC 2005, which is 1.5% (8.1mm) of story height. Finally, (3) slab cracks were concentrated across the specific long-span slabs and along the slab-wall joints throughout the height of the model. The crack patterns of exterior walls indicate that the exterior walls were subjected to not only the bending moment but also the membrane actions in compression and tension due to the overturning moment. The crack patterns of the inner walls were mainly flexural with minor shear cracks.

Keywords: Reinforced Concrete, Wall, Residential building, Scale model, Earthquake simulation test

1. INTRODUCTION

The number of apartment housing units is more than 58% of the total number of housing units in Korea (KNSO 2010). These residential apartment buildings such as shown in Fig. 1.1 generally consist of high-rise reinforced concrete (RC) wall structures, and should be designed and constructed to resist the earthquake according to Korea Building Code (AIK 2005, 2009), and existing buildings not satisfying these codes should be evaluated and retrofitted. These high-rise wall-type or box-type structural systems are defined as a bearing wall system in the code, but the style of these RC structures is unique around the world and the seismic performance of these structures has been investigated with due interest, neither in Korea nor abroad, except a few studies such as by Wood 1991 and Kalkan 2008.

In this research, a 1:5 scale 10-story RC wall-type building model representative of these residential buildings was constructed (Hwang 2011) considering the capacity of the largest shaking table available in Korea. Then, the seismic performance of the high-rise residential building model is evaluated based on the results of earthquake simulation tests.

2. DESIGN AND CONSTRUCTION OF THE MODEL

The prototype for the experiment was chosen to represent the most typical design in Korea. The floor area of one family unit is 89m^2 and one story accommodates two family units, while the number of stories is 10 as shown in Fig. 2.1. Though the prototype was designed according to the old design code of Korea, AIK2000 (AIK 2000), this model will be evaluated based on the new seismic design code

KBC2005 (AIK 2005), since the levels of design loads as per AIK2000 were very similar to those as per KBC2005. Table 2.1 shows equations to estimate the base shear coefficient and fundamental period according to AIK2000 and KBC2005 (AIK 2005). Though the structural system in both the X and Y directions is assumed to be the bearing wall system with the use of R-factor, 3, the natural period in the X direction was estimated by assuming a RC moment frame with that in the Y-direction obtained by using the equation for “other structures” in the code as given in Table 2.1. The thickness of walls is 180mm or 160mm with that of slabs being 200mm. The reinforcement of the walls is two-layered and the steel ratio of the vertical reinforcement ranges from 0.34% to 0.90%, while the horizontal steel ratio was designed to be 0.29%.

Considering the capacity of the available shaking table (5m×5m) and the feasibility of model reinforcements, a 1:5 scale 10–story building model was chosen. The weight of the 1:5 scale true replica model was estimated to be 851kN. However, because this weight exceeds the maximum pay-load capacity of the shaking table, 600kN, it was reduced again by half and acceleration was doubled by adopting the distorted model.

Dimensions of the experimental model are given in Fig. 2.2(a) and (b) with reinforcement details in Fig. 2.2(c). Since it was difficult to make the cross sections of the model reinforcement conform exactly to the similitude law, the yield forces rather than yield stresses were selected as the target (Lee and Woo 1998). The model reinforcements, D3 and Ø2, representing the D13 and D10 reinforcements with the nominal yield strength of 400MPa in prototype are shown in Fig. 2.3(a). Heat treatment in the vacuum furnace was conducted on these model reinforcements to obtain the target yield forces (D3: 1.99~2.58kN, D2: 1.12~1.45kN) in accordance with the similitude requirements, and the test results of the strain-force curve in tension are shown in Fig. 2.3(b). The model concrete was made using the maximum aggregate size of 4mm and the average 28-day compressive strength of 80 50mm*100mm cylinder specimens was 25.3Mpa with the design compressive strength in prototype being 24Mpa. Detailed information on the design and construction of the specimen is given in the reference (Hwang 2011).

Figure 1.1. Photo of RC residential buildings in Korea

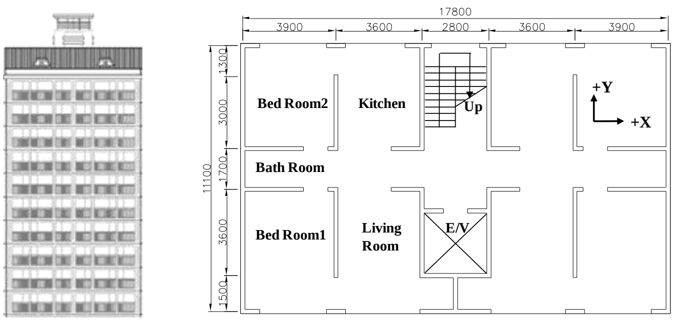

(a) Elevation (b) Plan

Figure 2.1. Design of prototype (unit: mm)

Table 2.1. Natural period and base shear coefficient

	AIK2000	KBC2005
Base Shear Coefficient (C_S)	$C_S = \frac{V}{W} = \frac{AI_E S}{1.2\sqrt{T}R} \le \frac{1.75AI}{R}$	$C_S = \frac{V}{W} = \frac{S_{D1}}{(R/I_E)T} \le \frac{S_{DS}}{R/I_E}$
	V: Base shear, W: Weight, A : Zone factor (0.11), I_E: Importance factor, S: Soil factor (1.2), R: Response modification factor (AIK: 3, KBC: 4.5), T: Fundamental period, S_{D1}, S_{DS}: Spectral accelerations at period 1sec and 0.2sec, respectively(0.234, 0.439)	
Natural Period	$T_a = C_t (h_n)^{3/4}$, $C_{t,x\text{-}dir.} = 0.0731$: RC MRF*, $C_{t,y\text{-}dir.} = 0.0488$: Others, h_x: height of structure	

MRF*: Moment Resisting Frame

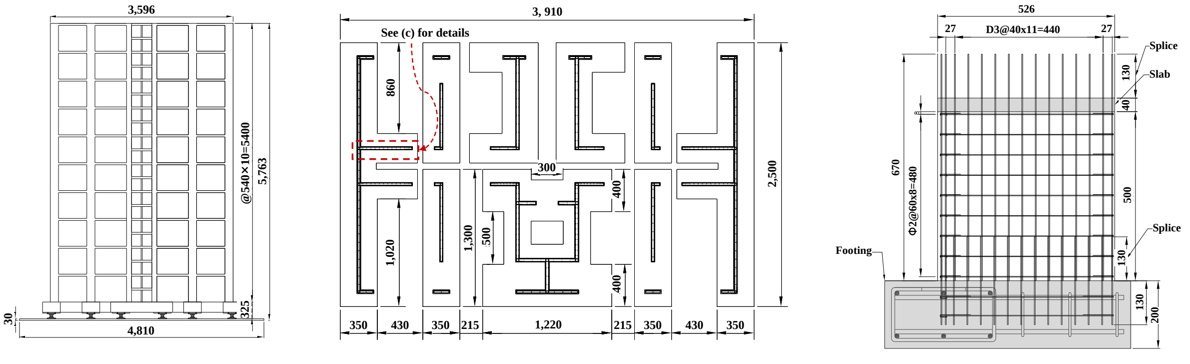

(a) Elevation (b) Base plan (c) Elevation of wall rebar

Figure 2.2. Dimensions of 1/5 scale model (unit: mm)

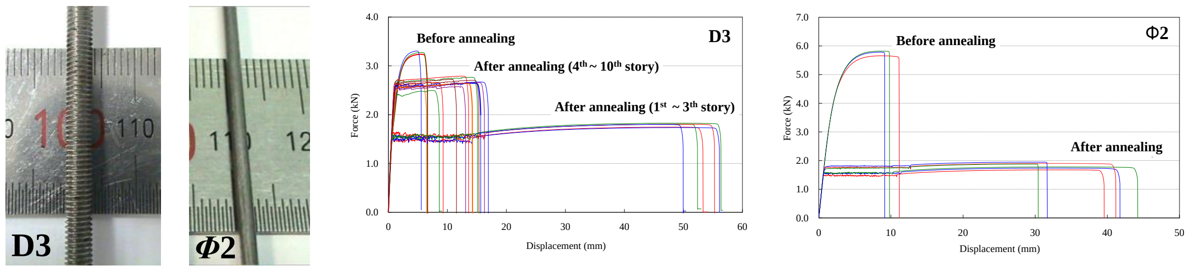

(a) D3 and ϕ 2 (b) Typical force versus strain relation of D3 and ϕ 2

Figure 2.3. Model reinforcement D3 and ϕ 2

3. EXPERIMENTAL SETUP, INSTRUMENTAION, AND TEST PROGRAM

The experimental set-up and instrumentation to measure displacements, accelerations, and forces are shown in Fig. 3.1. To measure lateral drifts and accelerations, displacement transducers and accelerometers were installed and the lateral drifts at the top and bottom of an independent steel post were measured at the corner of the shaking table to check the overturning movement of the shaking table itself in Fig. 3.1(a). Instrumentation to measure shear and flexural deformations was devised at the first and second stories.

In addition, the normal strain distributions in the plastic hinge regions of the walls were measured. Also, the displacement transducers were installed to measure the flexural out-of-plane deformation of the slab. Load cells were installed beneath the footings to measure the two directional shear forces and the axial force as shown in Fig. 3.1(b). The overview of experimental set-up is given in Fig. 3.1(c).

The input accelerograms for earthquake simulations were based on the recorded 1952 Taft N21E (X direction) and Taft S69E (Y direction) components. Because the weight of the model was reduced to be half of the true replica model considering the capacity of shaking table, the input accelerogram was formulated by compressing the time axis with the scale factor of $1/\sqrt{10}$ and by amplifying the acceleration with the scale factor of two. Steel blocks as shown in Fig. 3.1(a) were attached to the model to compensate the difference between the weight of the model itself and that required as per the similitude law. The test program is given in Table 3.1. X, Y, and XY in the designation of each test mean that the excitations were implemented in the X direction only, in the Y direction only, and in the X and Y directions simultaneously, respectively.

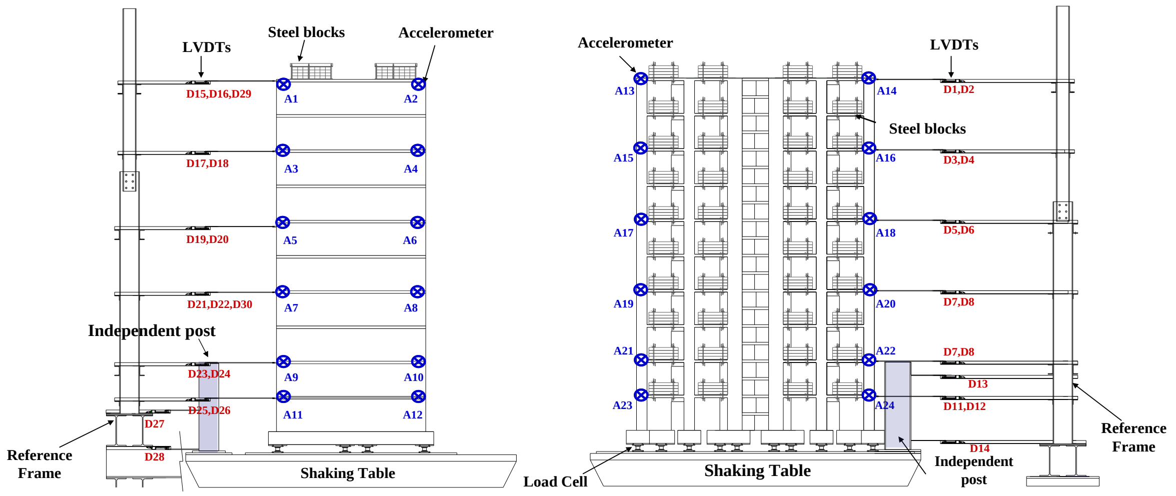

(a) Displacement transducers and accelerometers

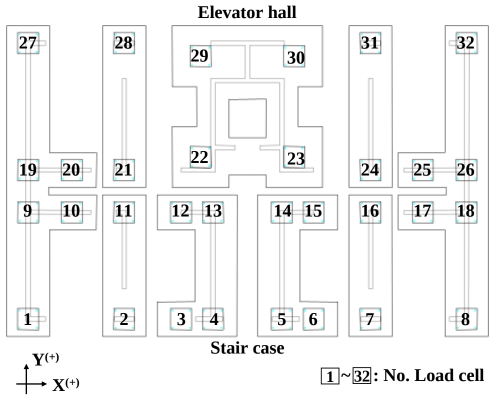

(b) Footings of walls and positions of load cells at base

(c) Overview of experimental set-up

Figure 3.1. Instrumentation

Table 3.1 Test Program

Test	Peak Ground Acceleration (PGA) (unit: g)				Return Periods in Korea (years)
	Input		Output		
	X-dir	Y-dir	X-dir	Y-dir	
0.035XY	0.035	0.040	0.070	0.070	
0.070X	0.070	–	0.089	–	
0.070Y	–	0.080	–	0.104	
0.070XY	0.070	0.080	0.068	0.110	
0.140X	0.140	–	0.172	–	50
0.140Y	–	0.161	–	0.152	
0.140XY	0.140	0.161	0.137	0.142	
0.308X	0.308	–	0.275	–	500
0.308XY	0.308	0.352	0.237	0.311	
0.374X	0.374	–	0.292	–	Design Earthquake (DE)
0.374XY	0.374	0.431	0.316	0.450	
0.60X	0.60	–	0.523	–	2400 MCE*
0.60XY	0.60	0.691	0.525	0.642	

MCE*: Maximum Considered Earthquake

4. TEST RESULTS AND OBSERVATIONS

4.1 Global responses

Fig. 4.1(a) compares design spectra as per KBC 2005 and response spectra obtained using the input and output accelerograms of shaking table excitations. The response spectra for the shake table output corresponding to the MCE (0.60XY) and the DE (0.374XY) simulate well the design spectra. Fig. 4.2 shows the time histories of roof drift, base shear, and overturning moment (OTM) under the MCE (0.60XY). The histories of shear force and OTM derived from load cells do not match exactly those derived from inertia forces as shown in Fig. 4.2(c), (d), (e), and (f) because some load cells did not function well and those data were excluded. Notwithstanding this fault, the data obtained from the load cells will be used to analyze the test result later. The maximum value of base shear coefficients (C_S) derived from the inertia force under 0.374XY and 0.60XY are in between design spectra corresponding to the values of response modification factors (*R*), 1 and 3 in Fig. 4.1(b). The demand under the MCE is approximately 1.5 times larger than that under the DE. Fig. 4.3 shows the vertical distribution of lateral drifts and accelerations along the height of the structure. Under 0.60XY, the maximum displacement in the X direction was 29.6mm and 1.4 times larger than the Y directional displacement (21.9mm). The shapes of lateral drifts are mainly that of the first mode with the shapes of lateral acceleration being almost uniform along the height of the model.

White noise tests were conducted before and after each level of earthquake simulation tests to measure the fundamental periods of the model. Fig. 4.4 shows the change of natural periods throughout the tests. The empirical predictions of the fundamental period, 0.27s in the X direction and 0.18s in the y direction for the RC MRF and other structures, respectively, as per KBC2005 match reasonably the test results. Fig. 4.5 shows the change of the base shear coefficient (C_S) and roof drift obtained throughout the tests. The nonlinear relation between the base shear and the roof drift can be clearly noticed with the over-strength factors under the DE (0.374XY) being approximately 2.0 in the X direction and 1.5 in the Y direction, respectively. Fig. 4.6 shows the distribution of inter-story drift (ID) under the DE (0.374XY). The maximum inter-story drift is 1.8mm in the X direction and 1.85mm in the Y direction at the first story. It can be found that these ID's are significantly smaller than the ID limit given in KBC2005, which is 1.5% (8.1mm) of story height (540mm). Fig. 4.7 shows hysteresis curves between the base shear and roof drift. The hysteresis curve under 0.140XY shows the linear behaviour. The curves under the DE (0.374XY) show the nonlinear behaviour in a limited amount, and the curves under the MCE (0.60XY) reveal large energy dissipation through the inelastic behaviour and significant losses of stiffness, which are 60% in the X direction and 39% in the Y direction when compared with the case of the test 0.140XY. It is noticed, in particular, that the structure experienced very large strength drop and partial failure after the peak response (237kN) in the Y direction in test 0.60XY.

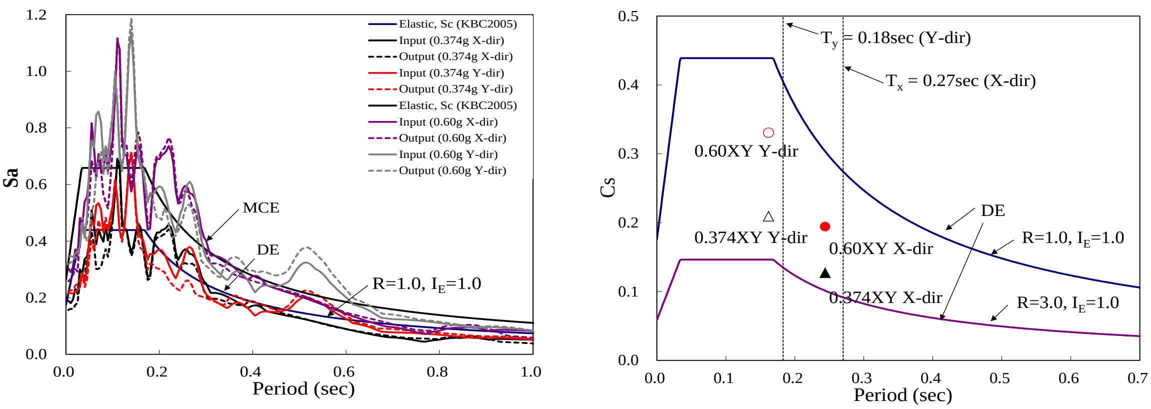

(a) Design and shake-table response spectra (b) Base shear coefficients (C_S)

Figure 4.1. KBC 2005 design and shake-table response spectra

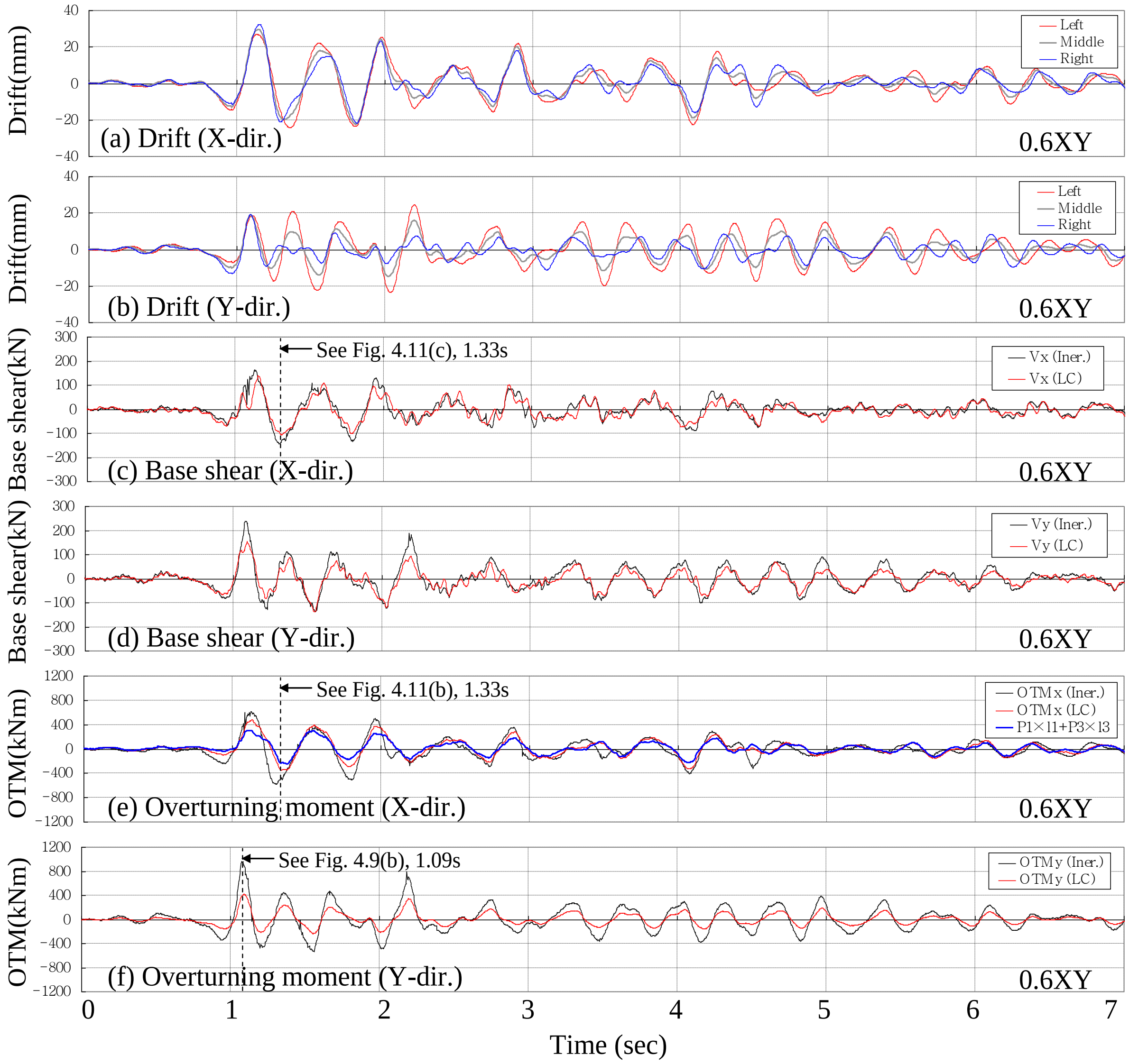

Figure 4.2. Time history of roof drift, base shear, and OTM (0.6XY)

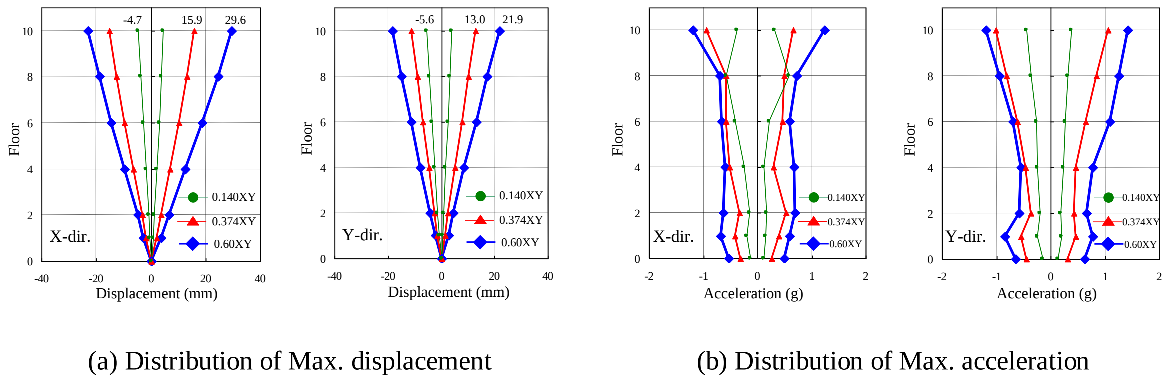

Figure 4.3. Distribution of maximum lateral displacement and acceleration

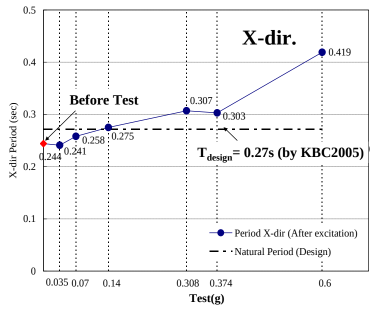

(a) Natural period (X-dir.)

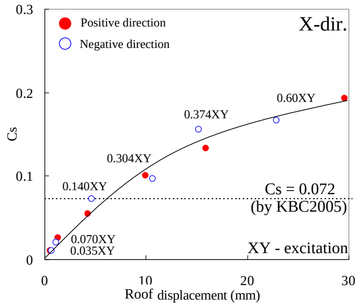

(a) C_S (X-dir.)

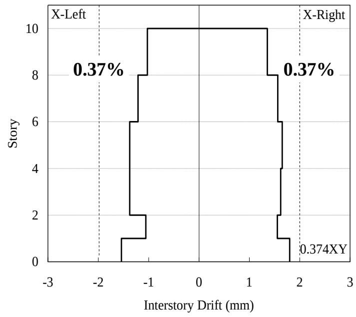

(a) ID (X-dir.)

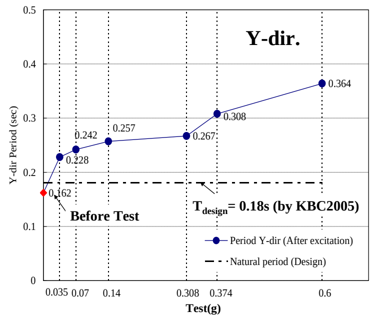

(b) Natural period (Y-dir.)

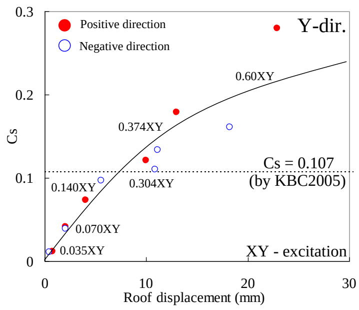

(b) C_S (Y-dir.)

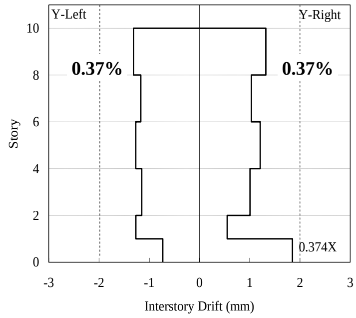

(b) ID (Y-dir.)

Figure 4.4. Natural period by white noise tests

Figure 4.5. Base shear coefficient (C_S) versus roof drift

Figure 4.6. Interstory drift (0.374XY)

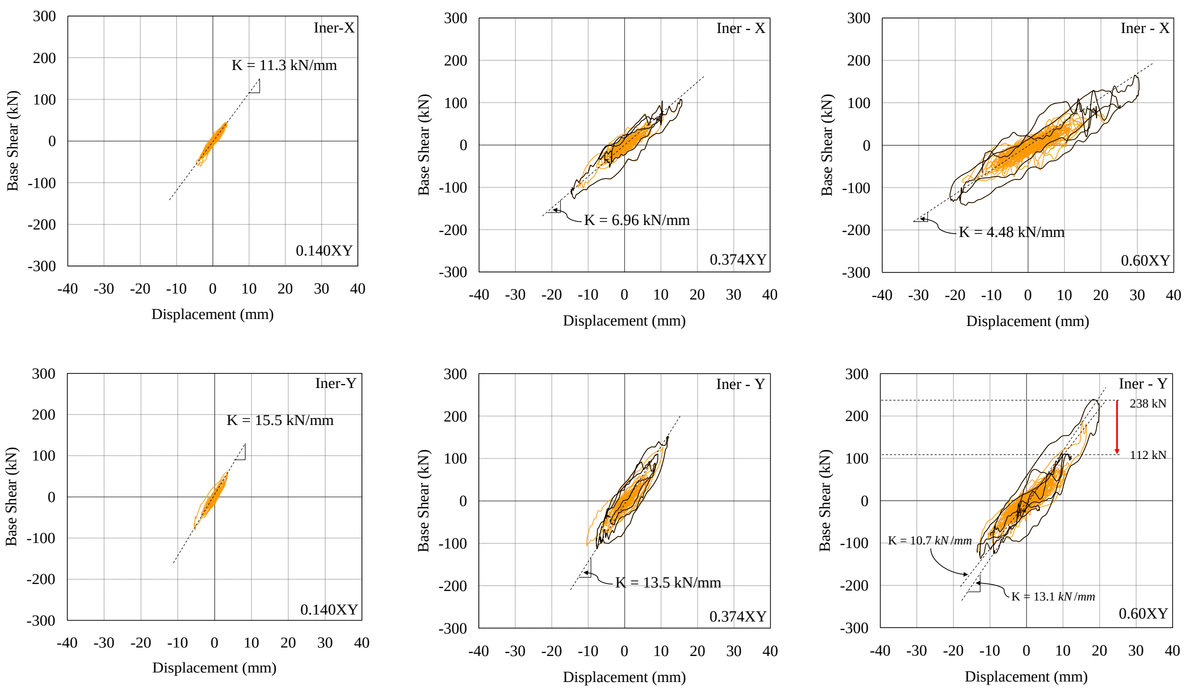

(a) 0.140XY (b) 0.374XY (c) 0.60XY

Figure 4.7. Base Shear versus roof drift

4.2 Crack pattern and resistance mechanism

Fig. 4.8(a) shows the upper-side views of the crack pattern on the roof and third-floor slab. Cracks were concentrated across the long-span slab and along the slab-wall joint in the Y direction. Most of the floors showed crack patterns similar to that of the third-floor slab. Fig. 4.8(b) demonstrates the overall view of the crack pattern in the bottom side of slabs. Also, it is noticeable that the end exterior wall in the Y direction has many horizontal cracks penetrating almost the full length of the walls at the lower stories as shown in Fig. 4.8(c). The horizontal cracks in walls indicate that the walls were subjected to not only the flexural bending but also the membrane action in tension or compression. Fig. 4.9(a) shows the crack patterns of exterior walls in the X direction, while Fig. 4.9(b) reveals the distribution of axial forces at load cells at the instant when the model was subjected to the maximum OTM in the Y direction. Fig. 4.9(a) indicates that the exterior walls are mainly subjected to the membrane forces in compression and tension due to the OTM. Fig. 4.10 shows the crack patterns of the inner walls, which are mainly flexural with minor shear cracks.

The reason for the crack patterns in the slabs and the walls can be explained with the formulation of the resistance mechanism of the model to the earthquake ground excitations as follows:(1) The whole structure can be divided into three portions of lateral force resisting vertical elements or cantilevers (A, B, and C part) as shown with shades in Fig 4.11(a). (2) The external OTM, $\sum F_i h_i$, is resisted by the sum of the base moments, $\sum M_i$, and the sum of the values of the axial force multiplied by the arm length, $\sum P_i l_i$, in other words, $\sum F_i h_i = \sum M_i + \sum P_i l_i$. (3) The external lateral forces, $\sum F_i$, is resisted by the sum of the base shears $\sum V_i$, that is, $\sum F_i = \sum V_i$. The values of base axial forces, base moments, and base shears for the three main portions of the structure at the instant of the maximum overturning moment (See Fig 4.2(c) and (e).) obtained from load cells are shown in Fig. 4.11(b) and (c). Approximately 70% of the total OTM is resisted by the component $\sum P_i l_i$ due to the axial force resistance of the outer walls, while over 90% of the total base shear is resisted by the central portion of the structure, i.e. that of the walls of the elevator hall and stair case.

The sum of the estimated shear capacities at the plastic hinges of slabs along the height of the model as shown in Fig. 4.11(a), $P_{capacity} = \sum v_i$, is 105kN, with the demand value of $P_{demand} = P_1$, 135kN, obtained by summing the axial forces measured in the corresponding load cells. This large axial force demand, P_{demand}, compared with $P_{capacity}$, explains the reasons for the occurrence of the similar crack patterns in the long-span slabs all along the height of the model as well as the horizontal cracks at the bottom portions of the exterior walls.

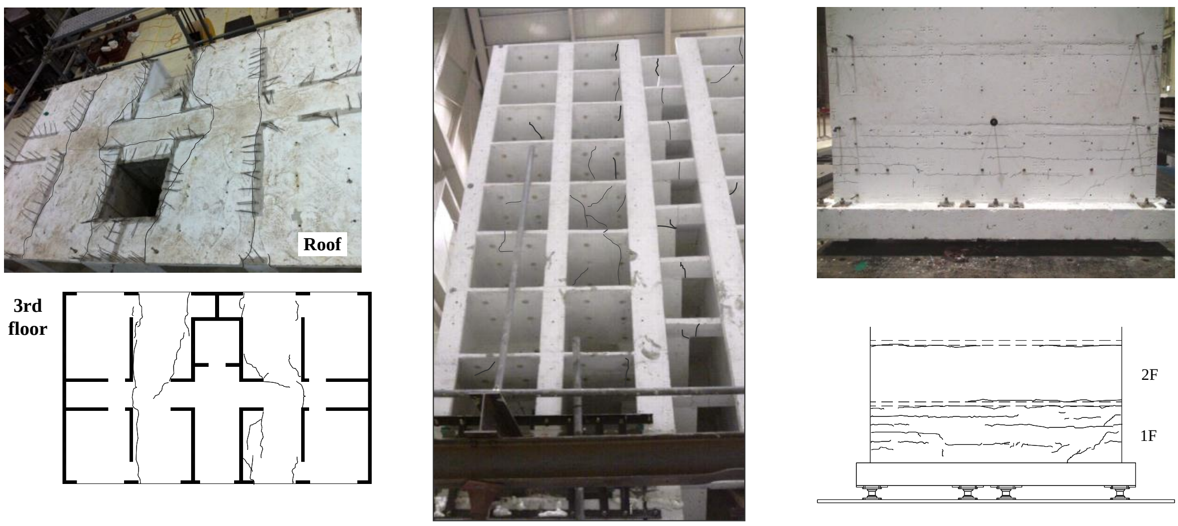

(a) View to the upper sides of roof and 3rd floor slab

(b) View to the undersides of slabs

(c) Exterior wall in Y direction

Figure 4.8. Overall crack patterns

(a) Exterior wall in X direction (b) Axial forces in load cells

Figure 4.9. Crack pattern in ext. walls in X-dir. and axial forces at load cells at instant of max. OTM in Y dir.

(a) View point (b) View A (c) View B (d) View C

Figure 4.10. Crack patterns in critical interior walls in the Y direction

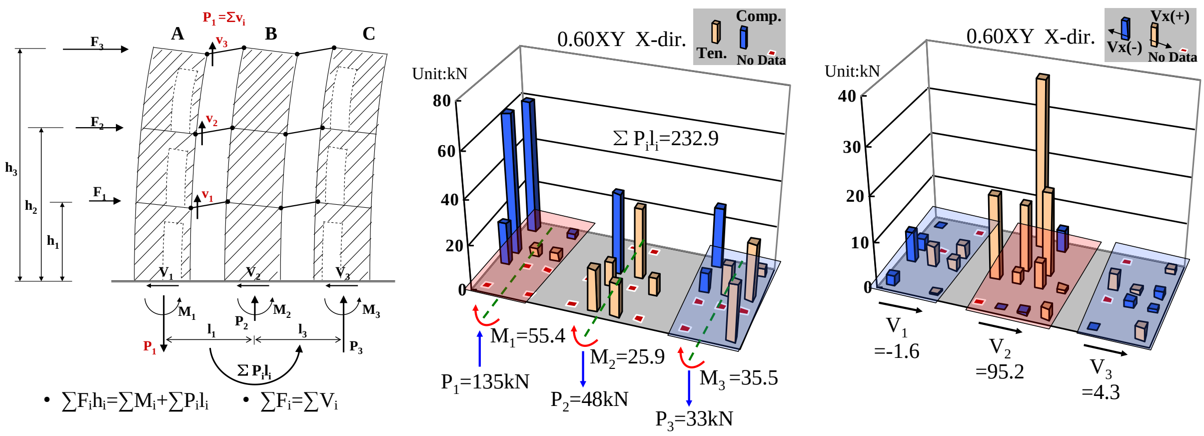

(a) Equilibrium in resistance (b) OTM (kNm) (axial forces in load cells) (c) Base Shear (kN) (X-dir. shear in load cells)

Figure 4.11. X-direction resistance in OTM and shear

5. CONCLUSIONS

The following conclusions are drawn based on the analysis of test results:

(1) The empirical predictions of the fundamental period, 0.27s in the X direction and 0.18s in the y direction for the RC MRF and other structures, respectively, as per KBC2005, match reasonably the test results.

(2) The values of base shear coefficient (C_S) under 0.374XY (DE) and 0.60XY (MCE) are in between design spectra corresponding to the values of response modification factors (R), 1 and 3. The demand under the MCE is generally 1.5 times larger than that under the DE. The nonlinear relationship between the base shear coefficient and the roof drift can be noticed with the over-strength factors

under the DE (0.374XY) being approximately 2.0 in the X direction and 1.5 in the Y direction, respectively, when compared with the design seismic load.
(3) The hysteretic curves between the base shear and roof drift under the DE (0.374XY) show the nonlinear behaviour in a limited amount, and the curves under the MCE (0.60XY) reveal a large energy dissipation through the inelastic behaviour and significant losses of stiffness, which are 60% in the X direction and 39% in the Y direction when compared with the case of the test 0.140XY. It is noticed, in particular, that the structure experienced very large strength drop and partial failure after the peak response in the Y direction in test 0.60XY.
(4) The maximum inter-story drift (ID) is 1.8mm in the X direction and 1.85mm in the Y direction at the first story under the DE (0.374XY). It can be found that these ID's are far smaller than the ID limit given in KBC 2005, which is 1.5% (8.1mm) of story height.
(5) Slab cracks were concentrated across the long-span slab and along the slab-wall joint all along the height of the model. The crack patterns of exterior or outer walls indicate that these walls were mainly subjected to the flexural bending as well as to the membrane actions in compression and tension due to the OTM. The crack patterns of the inner walls were mainly flexural with minor shear cracks.
(6) In the X direction, approximately 70% of the total OTM is resisted by the axial force resistance of the outer walls, while over 90% of the total base shear is resisted by the central portion of the structure, i.e. that of the walls of the elevator hall and stair case. This resistance mechanism of the structures explains clearly the reason for the observed crack patterns.

ACKNOWLEDGEMENT

The research presented herein was supported by the National Research Foundation of Korea through the contract No.2010-0000789.

REFERENCES

Architectural Institute of Korea. (2001). AIK2000, Seoul, Korea.

Architectural Institute of Korea. (2005). Korean Building Code (KBC 2005), Seoul, Korea.

Hwang, S. J., Lee, K. B., Kang, C. B., Lee, H. S., Lee, S. H., and Oh, S. H. (2011). Design and Construction of a 1:5 Scale 10-Story R.C. Apartment Building Model for Earthquake Simulation Tests. Journal of the Earthquake Engineering Society of Korea (in Korean). **15:6**, 67-80.

Kalkan, E., and Yuksel, S.B. (2008). Pros and Cons of Multistory RC Tunnel-Form (Box-type) Buildings. Journal of the Structural Design of Tall and Special Buildings. **17**, 601-617.

Korea National Statistical Office (2010), Population and Housing Census 2010. (in Korean).

Lee, H. S. and Woo, S. W. (1998). An experimental study on the similitude in structural behaviors for small-scale modeling of reinforced concrete structures. 6th U.S. National Conference on Earthquake Engineering. **Paper No. 308**.

Wood, S. L., Stark, R., and Greer, S.A. (1991). Collapse of Eight-Story RC Building during 1985 Chile Earthquake. Journal of Structural Engineering. **117:2**.